



# CHORUS

This is the accepted manuscript made available via CHORUS. The article has been published as:

## Onsager reciprocity relation for ballistic phonon heat transport in anisotropic thin films of arbitrary orientation

Geoff Wehmeyer, Andrea D. Pickel, and Chris Dames

Phys. Rev. B **98**, 014304 — Published 16 July 2018

DOI: [10.1103/PhysRevB.98.014304](https://doi.org/10.1103/PhysRevB.98.014304)

# An Onsager reciprocity relation for ballistic phonon heat transport in anisotropic thin films of arbitrary orientation

Geoff Wehmeyer<sup>1</sup>, Andrea D. Pickel<sup>1</sup>, and Chris Dames<sup>1</sup>

<sup>1</sup>*Department of Mechanical Engineering, University of California, Berkeley, California, United States*

---

## Abstract

A classic Onsager reciprocity relation for Fourier heat conduction in the absence of magnetic fields states that the thermal conductivity tensor in bulk anisotropic solids is symmetric. However, since Fourier’s law fails in thin dielectric films due to ballistic phonon transport effects, it is natural to ask whether an analogous Onsager relation can be identified in the boundary scattering regime. To answer this question, we solve the Boltzmann transport equation (BTE) under the relaxation time approximation for in-plane and cross-plane heat transport for thin films with anisotropic phonon dispersion relations and scattering rates. We use these BTE solutions to show that the thermal conductivity tensor of thin films is symmetric from the diffusive regime through the boundary scattering regime. We illustrate this reciprocity by calculating thermal conductivity suppression functions for a model anisotropic material. We compare our BTE solution to previous atomistic simulations of arbitrarily aligned graphite thin films, and use published first-principles calculations to model anisotropic in-plane heat flow in aligned black phosphorus. Our derivation shows how Onsager reciprocity for anisotropic heat conduction extends into the boundary scattering regime, and reduces the number of independent measurements required to fully characterize heat transport in anisotropic thin films.

---

## I. INTRODUCTION

Fourier’s law breaks down in dielectric thin films due to ballistic phonon transport effects, which become important when the film thickness  $t$  is comparable to or less than the phonon’s intrinsic mean free path  $\Lambda$ . The breakdown of Fourier’s law leads to a reduction in the thermal conductivity  $\kappa$  compared to the bulk value  $\kappa_{bulk}$ . Boltzmann transport equation (BTE) models have been developed [1–6] to quantify this thin film boundary scattering suppression in materials that have phonon dispersion relations and scattering rates of sufficiently high symmetry such that the heat flux  $\mathbf{q}$  is antiparallel to the temperature gradient  $\nabla T$ . For example, these BTE models are used to describe heat transport in silicon thin films [7–10], since silicon has a relatively high-symmetry diamond cubic crystal structure. However, for arbitrarily aligned materials with anisotropic dispersions and scattering rates,  $\mathbf{q}$  is no longer necessarily antiparallel to  $\nabla T$ , an effect described by off-diagonal terms in the  $\kappa$  tensor. These arbitrarily

aligned conditions can be found in thin films with low-symmetry monoclinic or triclinic unit cells [11–18], as well in films which have higher symmetry unit cells (*e.g.* orthorhombic) but have temperature gradients imposed in a low-symmetry direction [19–23]. Particular examples of recent thermal interest include the phase-change material vanadium dioxide ( $\text{VO}_2$ ) in the monoclinic phase [24,25], the layered material black phosphorus (which displays anisotropic in-plane thermal properties) [26], and thermoelectric materials such as SnSe [27] or  $\text{Bi}_2\text{Te}_3$  [28]. Being able to predict the boundary scattering effects on the thermal properties of these materials is important for interpretation of novel transport physics [24] and for applications in waste heat scavenging [29]. In addition, other arbitrarily aligned materials have been investigated for applications in heat flux sensing and transverse thermoelectric cooling [23,30].

In the diffusive regime where Fourier’s law applies, an important Onsager reciprocity relation for arbitrarily aligned anisotropic materials [31,32] mandates that the  $\kappa$  tensor is symmetric in the absence of a magnetic field. This prototypical relation dates back to Onsager’s first work on reciprocity [31] and fundamentally arises from the microscopic time reversal symmetry of the macroscopically irreversible diffusion process. However, this diffusive Onsager relation has not been theoretically or experimentally extended into the thin film boundary scattering regime where Fourier’s law breaks down due to ballistic phonon effects. In contrast, well-known examples of ballistic reciprocity can be found in the four-point probe conductance relations from the electrical domain [33,34]. These electrical results, however, are not easily modified to model the ballistic phonon transport of the present work, because the electrical four-point probe relations are derived from the Landauer-Büttiker formalism, while thin film phonon boundary scattering is analyzed using the Boltzmann equation.

Here, we identify a generalized version of the Onsager reciprocity relation by using BTE solution to show that the  $\kappa$  tensor is symmetric from the diffusive regime through the boundary scattering regime for arbitrarily aligned anisotropic thin films. We present an example calculation of the thin film reciprocity relation for a model material with an anisotropic Debye dispersion relation, and compare our BTE solutions to molecular dynamics simulations [35] of arbitrarily aligned graphite thin films. As a further case study, we combine a tensor transformation result from our BTE solutions with previously published first-principles calculations [6] to model thermal transport in thin-film black phosphorus, a layered material with anisotropic in-plane thermal conductivities. Our BTE solutions extend Onsager’s reciprocity relation for heat conduction into the boundary scattering regime, and the reciprocity relation reduces the number of independent measurements required to fully characterize heat transfer in anisotropic thin films.

## II. THEORY

### A. Boltzmann transport equation

We begin by deriving BTE solutions for heat transport in arbitrarily aligned anisotropic thin films. Under the relaxation time approximation, the steady-state phonon BTE without internal energy generation is

$$\mathbf{v}_k \cdot \nabla f_k = -\frac{f_k - f_{0,k}}{\tau_k}, \quad (1)$$

where  $\nabla$  is the gradient in real space, the subscript  $\mathbf{k}$  denotes the phonon wavevector for a given polarization,  $\mathbf{v}_k$  and  $\tau_k$  are respectively the mode-dependent group velocity and bulk relaxation time,  $f_k$  is the distribution function (initially unknown), and the equilibrium Bose-

Einstein distribution function  $f_{0,k} = \left( \exp\left(\frac{\hbar\omega_k}{k_B T}\right) - 1 \right)^{-1}$ . Note that for simplicity of presentation,

we suppress the index labeling the phonon polarization for all mode-dependent quantities, but this is understood to be contained within the symbol  $\mathbf{k}$ . The phonon angular frequency is  $\omega_k$ ,  $\hbar$  is the reduced Planck constant,  $k_B$  is the Boltzmann constant, and  $T$  is the unknown local temperature.

The local heat flux vector is

$$\mathbf{q} = \frac{1}{V} \sum_{\mathbf{k}} \hbar\omega_k \mathbf{v}_k f_k, \quad (2)$$

where  $V$  is the volume of the sample. In Eq. (2) and throughout this paper, a summation over  $\mathbf{k}$  also implies a sum over polarizations. Conservation of energy dictates that at steady state with no heat generation,  $\nabla \cdot \mathbf{q} = 0$ . Taking the gradient of Eq. (2), noting that  $\nabla \cdot \mathbf{v}_k = 0$  for a homogeneous material, and substituting for  $\mathbf{v}_k \cdot \nabla f_k$  using the BTE (Eq. (1)), the conservation of energy requirement becomes

$$\sum_{\mathbf{k}} \frac{\hbar\omega_k}{\tau_k} (f_k - f_{0,k}) = 0. \quad (3)$$

We will obtain BTE solutions for the two different scenarios of imposed temperature differences in the cross-plane direction and an in-plane direction. In both cases, we will use the recently developed deviational form of the Boltzmann equation [4,36]. In the deviational BTE, we consider small temperature differences, such that at any spatial location the difference between the actual temperature  $T$  and the reference Fourier temperature profile  $T_r$  is much smaller than the magnitude of  $T$ . The deviational BTE solution represents the linear response of the BTE, and is equivalent to neglecting the temperature dependence of microscopic quantities such as the modewise specific heats.

## B. Cross-plane temperature difference

We first consider a cross-plane temperature difference imposed across a thin film of thickness  $t$ , shown in Fig. 1(a). The bottom black surface ( $y = 0$ ) is at a hot temperature  $T_h$ , and the top black surface ( $y = t$ ) is at a cold temperature  $T_c$ , and thus the cross-plane Fourier temperature profile is  $T_{r,y} = T_h - (T_h - T_c)(y/t)$ . We apply periodic boundary conditions in the  $\hat{x}$  and  $\hat{z}$  directions, so the only gradients in  $f_{\mathbf{k}}$  and  $T$  are in the  $\hat{y}$  direction; however, for crystals of sufficiently low symmetry, the temperature difference in  $\hat{y}$  induces heat flows in orthogonal directions ( $\hat{x}, \hat{z}$ ).

We solve for the cross-plane deviational energy distribution function  $g_{\mathbf{k}} \equiv \hbar\omega_{\mathbf{k}}(f_{\mathbf{k}} - f_{\mathbf{k},0}(T_{r,y}))/C_{\mathbf{k}}(T_h - T_c)$ , where  $C_{\mathbf{k}} \equiv \hbar\omega_{\mathbf{k}} \frac{\partial f_{\mathbf{k},0}}{\partial T}$  is the modewise specific heat. We also introduce the dimensionless parameters  $\eta \equiv y/t$  and  $\lambda_{\mathbf{k},y} \equiv \Lambda_{\mathbf{k},y}/t$ . Here, the second subscript  $y$  indicates the vector mean free path has been projected along  $\hat{y}$ , that is,  $\Lambda_{\mathbf{k},y} \equiv (\mathbf{v}_{\mathbf{k}} \cdot \hat{y})\tau_{\mathbf{k}}$ . Due to this projection,  $\Lambda_{\mathbf{k},y}$  is positive (negative) for phonons travelling with group velocities along  $+\hat{y}$  ( $-\hat{y}$ ). Expressing Eq. (1) in terms of  $g_{\mathbf{k}}$ , and noting that  $\hbar\omega_{\mathbf{k}}[f_{\mathbf{k},0}(T) - f_{\mathbf{k},0}(T_{r,y})] = C_{\mathbf{k}}(T - T_{r,y})$  for small temperature differences, the BTE becomes

$$\lambda_{\mathbf{k},y} \frac{dg_{\mathbf{k}}}{d\eta} + g_{\mathbf{k}} = \lambda_{\mathbf{k},y} + \Delta T_y(\eta), \quad (4)$$

where  $\Delta T_y(\eta) \equiv (T(\eta) - T_{r,y}(\eta))/(T_h - T_c)$  is the (currently undetermined) dimensionless deviational cross-plane temperature profile due to the imposed temperature difference in  $y$ . Using an integrating factor, we obtain the integral forms of Eq. (4) as

$$g_{\mathbf{k}}^+(\eta) = g_{\mathbf{k},0}^+ \exp\left(-\frac{\eta}{\lambda_{\mathbf{k},y}}\right) + \int_{\eta'=0}^{\eta} [\lambda_{\mathbf{k},y} + \Delta T_y(\eta')] \exp\left(-\frac{\eta - \eta'}{\lambda_{\mathbf{k},y}}\right) \frac{d\eta'}{\lambda_{\mathbf{k},y}} \quad (5)$$

$$g_{\mathbf{k}}^-(\eta) = g_{\mathbf{k},1}^- \exp\left(\frac{1-\eta}{\lambda_{\mathbf{k},y}}\right) - \int_{\eta'=1}^{\eta} [\lambda_{\mathbf{k},y} + \Delta T_y(\eta')] \exp\left(-\frac{\eta - \eta'}{\lambda_{\mathbf{k},y}}\right) \frac{d\eta'}{\lambda_{\mathbf{k},y}}. \quad (6)$$

Here  $g_{\mathbf{k}}^+(\eta)$  is the distribution function for phonons travelling upward ( $\lambda_{\mathbf{k},y} > 0$ ), and  $g_{\mathbf{k}}^-(\eta)$  is the distribution function for phonons travelling downward ( $\lambda_{\mathbf{k},y} < 0$ ). Using the boundary condition  $f_{\mathbf{k}} = f_{\mathbf{k},0}(T_{r,y})$  for all phonons emitted from a wall, the integration constants are simply  $g_{\mathbf{k},0}^+ = g_{\mathbf{k},1}^- = 0$ .

Now we implement the energy conservation requirement. Substituting the definition of  $g_{\mathbf{k}}$  into Eq. (3), we have

$$\Delta T_y(\eta) = \left( \sum_{\mathbf{k}} \frac{C_{\mathbf{k}}}{\tau_{\mathbf{k}}} \right)^{-1} \left( \sum_{\mathbf{k}} \frac{C_{\mathbf{k}}}{\tau_{\mathbf{k}}} g_{\mathbf{k}} \right). \quad (7)$$

Substituting the integral forms of the BTE (Eqs. (5) and (6)) into Eq. (7) yields an integral expression for the unknown  $\Delta T_y$ . This expression can be further simplified using the required inversion symmetries [37] of the phonon dispersion relation: time reversal symmetry mandates that  $C_{\mathbf{k}}$  is even and  $\mathbf{v}_{\mathbf{k}}$  is odd upon inversion of  $\mathbf{k}$ , even if the point group of the crystal's unit cell is non-centrosymmetric. We also restrict our attention to the most common phonon scattering processes (such as phonon-phonon or phonon-impurity scattering) that do not involve magnetic fields and thus obey time-reversal symmetry [31]. Therefore,  $\tau_{\mathbf{k}}$  is also even under inversion of  $\mathbf{k}$ . Using these inversion symmetries, we obtain an integral equation for the deviational temperature profile

$$\Delta T_y(\eta) = \left( \sum_{\mathbf{k}} \frac{C_{\mathbf{k}}}{\tau_{\mathbf{k}}} \right)^{-1} \sum_{\lambda_{\mathbf{k},y} > 0} \frac{C_{\mathbf{k}}}{\tau_{\mathbf{k}}} \lambda_{\mathbf{k},y} \left[ \exp\left(-\frac{1-\eta}{\lambda_{\mathbf{k},y}}\right) - \exp\left(-\frac{\eta}{\lambda_{\mathbf{k},y}}\right) + \int_{\eta'=0}^1 \Delta T_y(\eta') \exp\left(-\frac{|\eta-\eta'|}{\lambda_{\mathbf{k},y}}\right) \frac{d\eta'}{\lambda_{\mathbf{k},y}^2} \right]. \quad (8)$$

The notation in Eq. (8) indicates a summation over all modes that have  $\lambda_{\mathbf{k},y} > 0$ . To summarize this intermediate result, we have derived the temperature profile in response to a cross-plane temperature difference  $(T_h - T_c)$  applied at the boundaries. We will later use Eq. (8) to derive the reciprocity relation.

### C. In-plane temperature difference

We now move on to consider the conjugate problem of in-plane temperature differences along an arbitrarily selected in-plane direction  $\hat{x}$  for a thin film of thickness  $t$  and a large length  $L$ , as shown in Fig. 1(b). The traditional BTE approach for in-plane transport [1,2,4] never explicitly enforces energy conservation to find the temperature profile, but rather assumes that the temperature profile is always the in-plane Fourier reference temperature profile  $T_{r,x}(x) = T_h - (T_h - T_c)(x/L)$ . However, we will show that the temperature profile in arbitrarily aligned thin films can deviate from  $T_{r,x}$  due to ballistic effects, indicating that the energy conservation requirement  $\nabla \cdot \mathbf{q} = 0$  must be deployed to solve for the actual temperature profile.

The in-plane solution is very similar to the cross-plane procedure detailed above. We solve for the in-plane energy distribution function  $j_{\mathbf{k}} \equiv \hbar \omega_{\mathbf{k}} (f_{\mathbf{k}} - f_{\mathbf{k},0}(T_{r,x})) / C_{\mathbf{k}} (T_h - T_c)$ ,

where  $j_{\mathbf{k}}$  is analogous to  $g_{\mathbf{k}}$  from the cross-plane scenario. Introducing the dimensionless  $x$  location  $\zeta \equiv x/L$  and substituting into Eq. (1), the BTE becomes

$$\lambda_{\mathbf{k},x} \frac{dj_{\mathbf{k}}}{d\zeta} + \lambda_{\mathbf{k},y} \frac{dj_{\mathbf{k}}}{d\eta} + j_{\mathbf{k}} = \lambda_{\mathbf{k},x} + \Delta T_x, \quad (9)$$

where  $\lambda_{\mathbf{k},x} \equiv \Lambda_{\mathbf{k},x}/L$  and  $\Delta T_x(\eta) \equiv (T - T_{r,x}) / (T_h - T_c)$ . Since  $\lambda_{\mathbf{k},x} \ll \lambda_{\mathbf{k},y}$ , we drop the derivative involving  $\zeta$ , and Eq. (9) becomes a first order ODE for  $j_{\mathbf{k}}(\eta)$ .

The boundary conditions for in-plane transport should be conjugate to the cross-plane scenario boundary conditions. In the cross-plane solution, heat is allowed to flow along  $\hat{x}$  due to the temperature difference along  $\hat{y}$ . Similarly, for the in-plane solution, the boundary conditions must allow heat to flow along  $\hat{y}$  due to a temperature difference along  $\hat{x}$ . Therefore, we treat the bottom and top surfaces ( $y=0$  and  $y=t$ ) as black emitters maintained at  $T_{r,x}(x)$ . This choice of boundary conditions allows heat to leave the film through the top and bottom surfaces, thereby providing the correct conjugate behavior to the cross-plane scenario.

Proceeding analogously to the cross-plane case (see Appendix A for the intermediate details), we obtain an integral equation for the in-plane deviational temperature profile

$$\Delta T_x(\eta) = \left( \sum_{\mathbf{k}} \frac{C_{\mathbf{k}}}{\tau_{\mathbf{k}}} \right)^{-1} \sum_{\lambda_{\mathbf{k},y} > 0} \frac{C_{\mathbf{k}}}{\tau_{\mathbf{k}}} \lambda_{\mathbf{k},x} \left[ \exp\left(-\frac{1-\eta}{\lambda_{\mathbf{k},y}}\right) - \exp\left(-\frac{\eta}{\lambda_{\mathbf{k},y}}\right) + \int_{\eta'=0}^1 \Delta T_x(\eta') \exp\left(-\frac{|\eta-\eta'|}{\lambda_{\mathbf{k},y}}\right) \frac{d\eta'}{\lambda_{\mathbf{k},y} \lambda_{\mathbf{k},x}} \right]. \quad (10)$$

If the material has a mirror symmetry on reflection across the  $yz$  plane (i.e.  $\lambda_{\mathbf{k},x}$  is odd and  $\lambda_{\mathbf{k},y}$  is even upon taking  $k_x$  to  $-k_x$ ), the summation over the first two terms in the square bracket of Eq. (10) is zero. In that case, the trivial solution  $\Delta T_x(\eta) = 0$  results and no temperature gradients develop in the cross-plane direction  $y$ . This is the scenario for isotropic or aligned anisotropic thin films. However, a cross-plane temperature gradient can develop when the mirror symmetry is broken in the arbitrarily aligned scenario. Lastly, because the in-plane direction  $\hat{x}$  was arbitrarily designated, the results of this section are trivially modified for temperature differences applied in the orthogonal in-plane direction  $\hat{z}$  by relabeling the subscripts from  $x$  to  $z$  in Eq. (10).

#### D. Onsager reciprocity relation for thin film boundary scattering

We now use our BTE solutions to derive the central result of the paper, which is the generalized Onsager reciprocity relation for thin films with anisotropic dispersion relations or scattering. We will show that the  $\kappa$  tensor is symmetric from the diffusive regime through the boundary scattering regime. We note that even though Fourier's law itself breaks down in the ballistic regime, it is useful to generalize the thermal conductivity concept into the boundary

scattering regime by defining the elements of the  $\kappa$  tensor using the total heat flows, temperature differences, and sample dimensions. For example, the in-plane thermal conductivity  $\kappa_{xx}$  of thin films is conventionally defined [4] as  $\kappa_{xx} \equiv -Q'_x / (t \frac{dT}{dx})$ , where  $Q'_x \equiv t \int_0^1 q_x d\eta$  is the in-plane heat flow divided by the sample width in the  $\hat{z}$  direction  $w$ . In the diffusive regime where Fourier's law holds,  $\kappa_{xx} = \kappa_{xx,bulk}$ . However,  $\kappa_{xx}$  is suppressed below  $\kappa_{xx,bulk}$  in the boundary scattering regime where Fourier's law breaks down due to ballistic effects.

To prove that the  $\kappa$  tensor is symmetric, we need to determine the six off-diagonal components of the tensor. We begin by calculating  $\kappa_{xy}$ , defined as the ratio of  $Q'_x$  to the cross-plane temperature difference  $(T_h - T_c)$ . Substituting the definition of  $g_k$  into the definition of the heat flux (Eq. (2)) and dividing by  $(T_h - T_c)$ ,

$$\kappa_{xy} = \frac{1}{V} \sum_{\mathbf{k}} C_{\mathbf{k}} v_{\mathbf{k},x} t \int_0^1 g_{\mathbf{k}} d\eta. \quad (11)$$

We find  $\int_0^1 g_{\mathbf{k}} d\eta$  by integrating the BTE (Eq. (4)) from  $\eta = 0$  to 1 and re-arranging to obtain

$$\int_0^1 g_{\mathbf{k}} d\eta = -\lambda_{\mathbf{k},y} [g_{\mathbf{k}}(1) - g_{\mathbf{k}}(0) - 1] + \int_0^1 \Delta T_y(\eta) d\eta. \quad (12)$$

Here  $g_{\mathbf{k}}(0)$  and  $g_{\mathbf{k}}(1)$  are determined from the integral form of the BTE (Eqs. (5) and (6)) after applying the boundary conditions. Substituting into Eq. (11) after again using the inversion symmetry of the dispersion and scattering, we obtain an important final result for the off-diagonal conductivity

$$\begin{aligned} \kappa_{xy} = & \kappa_{xy,bulk} - \frac{2}{V} \sum_{\lambda_{\mathbf{k},y} > 0} \kappa_{\mathbf{k},xy} \lambda_{\mathbf{k},y} \left[ 1 - \exp\left(-\frac{1}{\lambda_{\mathbf{k},y}}\right) \right] \\ & - \frac{1}{V} \sum_{\lambda_{\mathbf{k},y} > 0} \kappa_{\mathbf{k},xy} \int_{\eta=0}^1 \Delta T_y(\eta) \left[ \exp\left(-\frac{1-\eta}{\lambda_{\mathbf{k},y}}\right) - \exp\left(-\frac{\eta}{\lambda_{\mathbf{k},y}}\right) \right] \frac{d\eta}{\lambda_{\mathbf{k},y}}. \end{aligned} \quad (13)$$

Here, we have introduced the modewise contribution to the off-diagonal thermal conductivity

$$\kappa_{\mathbf{k},xy} \equiv C_{\mathbf{k}} v_{\mathbf{k},x} v_{\mathbf{k},y} \tau_{\mathbf{k}}, \text{ such that the bulk off-diagonal thermal conductivity } \kappa_{xy,bulk} = \frac{1}{V} \sum_{\mathbf{k}} \kappa_{\mathbf{k},xy}.$$

In the diffusive regime where  $\lambda_{\mathbf{k},y} \ll 1$  for all phonons, the first term on the right hand side (RHS) of Eq. (13) dominates and we recover the Fourier result  $\kappa_{xy} = \kappa_{xy,bulk}$ . In the ballistic regime where  $\lambda_{\mathbf{k},y} \gg 1$ , the first two terms on the RHS combine to yield the ballistic

$$\text{conductivity } \kappa_{xy} = \frac{1}{V} \sum_{\lambda_{\mathbf{k},y} > 0} C_{\mathbf{k}} v_{\mathbf{k},x} t.$$

Interestingly, in both the diffusive and ballistic regimes, the last term in Eq. (13) including the deviational temperature profile is unimportant and we do not need to solve the integral equation for  $\Delta T_y$  (Eq. (8)). This can be seen by noting that in the diffusive regime,  $\Delta T_y$  is of order  $\lambda_y (\ll 1)$  and the third term in Eq. (13) is smaller than the first term by a factor of  $\lambda_y$ . In the ballistic regime,  $\Delta T_y$  is of order  $1/2$ , and the third term is smaller than the ballistic conductivity by a factor of  $1/\lambda_y$ . In the intermediate regime where  $\lambda_{\mathbf{k},y} \sim 1$ , all three terms contribute to  $\kappa_{xy}$ .

Now, we likewise calculate  $\kappa_{yx} \equiv Q'_y / (T_h - T_c)$ , where  $Q'_y \equiv L \int_0^1 q_y d\zeta$  is the cross-plane heat flow divided by  $w$  and  $(T_h - T_c)$  is the in-plane temperature difference. We will further manipulate  $Q'_y$  into a convenient form for the Onsager relation. First, we note that  $q_y$  is independent of position, which follows from the energy conservation requirement  $\nabla \cdot \mathbf{q} = 0$

and the large  $L$  stipulation that  $\frac{\partial q_x}{\partial x} = \frac{\partial q_y}{\partial x} = 0$ . Thus,  $Q'_y$  can equivalently be written as

$$Q'_y = L \int_0^1 q_y d\eta, \text{ since } \int_0^1 q_y d\eta = \int_0^1 q_y d\zeta = q_y. \text{ We choose to represent } Q'_y \text{ in this peculiar}$$

manner to facilitate later comparisons with  $Q'_x$  from the cross-plane scenario, where the integral over the dimensionless  $y$  location  $\eta$  arises naturally. Therefore, the off-diagonal

$$\text{conductivity } \kappa_{yx} = \frac{1}{V} \sum_{\mathbf{k}} C_{\mathbf{k}} v_{\mathbf{k},y} L \int_0^1 j_{\mathbf{k}} d\eta.$$

Proceeding similarly to the development of Eq. (13), we integrate the in-plane BTE (Eq. (9)) from  $\eta = 0$  to 1 to obtain an expression for  $\int_0^1 j_{\mathbf{k}} d\eta$ , and then determine  $j_{\mathbf{k}}(0)$  and  $j_{\mathbf{k}}(1)$  using the integral form of the BTE. Multiplying by  $C_{\mathbf{k}} v_{\mathbf{k},y}$ , summing over all modes, and using inversion symmetry, we obtain

$$\begin{aligned}\kappa_{yx} &= \kappa_{xy,bulk} - \frac{2}{V} \sum_{\lambda_{k,y}>0} \kappa_{k,xy} \lambda_{k,y} \left[ 1 - \exp\left(-\frac{1}{\lambda_{k,y}}\right) \right] \\ &\quad - \frac{1}{V} \sum_{\lambda_{k,y}>0} \kappa_{k,xy} \int_{\eta=0}^1 \Delta T_x(\eta) \left[ \exp\left(-\frac{1-\eta}{\lambda_{k,y}}\right) - \exp\left(-\frac{\eta}{\lambda_{k,y}}\right) \right] \frac{d\eta}{\lambda_{k,x}}.\end{aligned}\tag{14}$$

We have also leveraged the fact that by definition,  $\kappa_{xy,bulk} = \kappa_{yx,bulk}$  and  $\kappa_{k,xy} = \kappa_{k,yx}$ . Since the first two terms on the RHS of Eq. (14) for  $\kappa_{yx}$  are exactly the same as the first two terms on the RHS of Eq. (13) for  $\kappa_{xy}$ , subtracting and rearranging yields

$$\begin{aligned}\kappa_{xy} - \kappa_{yx} &= -\frac{tL}{V} \int_{\eta=0}^1 \Delta T_y(\eta) \left\{ \sum_{\lambda_{k,y}>0} \frac{C_k \lambda_{k,x}}{\tau_k} \left[ \exp\left(-\frac{1-\eta}{\lambda_{k,y}}\right) - \exp\left(-\frac{\eta}{\lambda_{k,y}}\right) \right] \right\} d\eta \\ &\quad + \frac{tL}{V} \int_{\eta=0}^1 \Delta T_x(\eta) \left\{ \sum_{\lambda_{k,y}>0} \frac{C_k \lambda_{k,y}}{\tau_k} \left[ \exp\left(-\frac{1-\eta}{\lambda_{k,y}}\right) - \exp\left(-\frac{\eta}{\lambda_{k,y}}\right) \right] \right\} d\eta.\end{aligned}\tag{15}$$

The terms in braces that multiply each of the deviational temperature profiles in Eq. (15) have already appeared in the integral solutions of the BTE (Eqs. (8) and (10)). Substituting those expressions into Eq. (15) and simplifying, we see that

$$\kappa_{xy} - \kappa_{yx} = \frac{tL}{V} \sum_{\lambda_{k,y}>0} \frac{C_k}{\tau_k \lambda_{k,y}} \left[ \int_{\eta=0}^1 \int_{\eta'=0}^1 \exp\left(-\frac{|\eta-\eta'|}{\lambda_{k,y}}\right) \left[ \Delta T_y(\eta) \Delta T_x(\eta') - \Delta T_y(\eta') \Delta T_x(\eta) \right] d\eta d\eta' \right].\tag{16}$$

The integrand of Eq. (16) is anti-symmetric upon the exchange of variables  $(\eta, \eta') \leftrightarrow (\eta', \eta)$ . Since the limits of integration are from 0 to 1 for both  $\eta$  and  $\eta'$ , we see that every contribution to the integral from  $(\eta, \eta')$  is exactly nulled by the corresponding contribution from  $(\eta', \eta)$  of equal magnitude but opposite sign. Therefore, regardless of the functional forms of  $\Delta T_y(\eta)$  and  $\Delta T_x(\eta)$ , Eq. (16) must always integrate to 0, and so

$$\kappa_{xy} = \kappa_{yx}.\tag{17}$$

Thus, we have found a principal result of this paper: a derivation of a thermal conductivity reciprocity relation from the BTE.

We now extend this ( $x \leftrightarrow y$ ) reciprocity relation to the other two pairs of off-diagonal terms in the  $\kappa$  tensor. First, we note that since our distinction between the two orthogonal in-plane directions  $(\hat{x}, \hat{z})$  was entirely arbitrary, the previous proof leading to Eq. (17) also shows that  $\kappa_{zy} = \kappa_{yz}$ . The last pair of off-diagonal thermal conductivities to compute from the BTE are the in-plane off-diagonal components  $\kappa_{zx}$  and  $\kappa_{xz}$ . In Appendix B, we follow a procedure

analogous to the development of Eqs. (11)-(17) to show that  $\kappa_{zx} = \kappa_{xz}$ . Therefore, the BTE solutions show that the thermal conductivity tensor is always symmetric for arbitrarily aligned anisotropic thin films.

Compared to the original diffusive Onsager relation, which was derived in the bulk regime and relies on the validity of Fourier's law [31], the BTE reciprocity relation is valid from the diffusive through the boundary scattering regime in which Fourier's law breaks down. Both reciprocity relations fundamentally arise from the time-reversal symmetry of the carrier dynamics [31], which are manifested in the inversion symmetry of the phonon dispersion and scattering rates.

### III. RESULTS AND DISCUSSION

#### A. Illustration and numerical validation of the Onsager relation

As a simple illustration of the reciprocity relation (Eq. (17)), we first consider heat transport in a model material with an anisotropic Debye dispersion relation [38]

$$\omega^2 = v_{ab}^2 k_{ab}^2 + v_c^2 k_c^2. \quad (18)$$

Here,  $v_{ab}$  and  $v_c$  ( $k_{ab}$  and  $k_c$ ) are the group velocities (wavevectors) in the  $\hat{ab}$  and  $\hat{c}$  directions of the crystal. The crystal is rotated by an angle  $\Psi$  in the  $xy$  plane; at  $\Psi = 0$ , the  $\hat{c}$  direction of the crystal is aligned with the  $\hat{y}$  direction of the film. Figure 2(a) shows the reciprocal space representation of the iso-frequency ellipsoid for this anisotropic Debye dispersion relation, and illustrates the fact that the group velocity vectors are normal to the iso- $\omega$  surface (phonon focusing). For simplicity, and to emphasize the impact of the anisotropic dispersion, we consider a single phonon polarization, a spherical first Brillouin zone, and focus on the high temperature limit where  $C_{\mathbf{k}} = k_B$  for all phonons. We also take the scattering to be gray ( $\tau_{\mathbf{k}} = \tau$  for all  $\mathbf{k}$ ).

To quantify the impact of boundary scattering on the off-diagonal thermal conductivities, we define the suppression functions  $S_{xy} \equiv \kappa_{xy} / \kappa_{xy,bulk}$  and  $S_{yx} \equiv \kappa_{yx} / \kappa_{yx,bulk}$ , which are the ratios of the actual BTE thermal conductivities to the bulk values. For the anisotropic Debye model considered here,  $S_{xy}$  and  $S_{yx}$  are functions of three dimensionless groups: the group velocity ratio  $v_{ab} / v_c$ , the tilt angle  $\Psi$ , and the dimensionless  $c$ -axis mean free path  $\lambda_c \equiv v_c \tau / t$ .

Figure 2(b) shows the suppression functions  $S_{xy}$  (points) and  $S_{yx}$  (lines) as functions of  $\lambda_c$  for  $\Psi = 30^\circ$  and three values of  $v_{ab} / v_c$ . We evaluated  $S_{xy}$  and  $S_{yx}$  numerically using two separate equations (Eq. (13) and Eq. (14)) and confirmed that  $S_{xy} = S_{yx}$  over all parameter

ranges considered (within 0.1% numerical precision). The fact that  $S_{xy} = S_{yx}$  for all  $v_{ab}/v_c$  and  $\lambda_c$  in Fig. 2(b) is a specific example of the general result  $\kappa_{xy} = \kappa_{yx}$  (Eq. (17)). In Fig. 2(b), we see that  $S_{xy}$  decreases for larger values of  $\lambda_c$ , representing the suppressed thermal transport due to boundary scattering. Interestingly, the difference in the suppression functions between  $v_{ab}/v_c = 0.1$  and  $v_{ab}/v_c = 3$  is relatively small despite the significant change in group velocity ratio, while increasing the velocity ratio to  $v_{ab}/v_c = 10$  shifts the suppression function curves to smaller  $\lambda_c$ . This occurs because for  $v_{ab}/v_c \gg 1$ , boundary scattering becomes more important for small  $\lambda_c$  due to the long mean free paths along the  $\hat{ab}$ -directions.

## B. Comparison with atomistic simulations: arbitrarily aligned graphite

We next compare our BTE solution for arbitrarily aligned anisotropic thin films to recently published non-equilibrium molecular dynamics (NEMD) simulations [35]. The NEMD simulations apply cross-plane temperature differences to graphite films of various thicknesses and basal plane alignments. To characterize the basal plane alignment we use the same convention as in Fig. 2 where the  $c$ -axis of graphite is tilted by an angle  $\Psi$  with respect to the  $\hat{y}$  direction of the thin film: for example,  $\Psi=0^\circ$  represents the scenario where the basal plane is parallel to the film boundaries.

In these NEMD thickness-convergence studies [35], the thermal conductivity was defined as  $\kappa_{yy,NEMD} \equiv -q_y / \frac{dT}{dy}$ , where the temperature gradient  $\frac{dT}{dy}$  within the film is smaller than the Fourier result  $(T_c - T_h)/t$  due to the temperature jump at the boundary between the thermal reservoirs and the sample. This definition is reasonable within the context of NEMD simulations where  $\frac{dT}{dy}$  is known, but in experiments where only  $q_y$ ,  $T_h - T_c$ , and  $t$  are measured, the typical definition used in our BTE solutions  $\kappa_{yy} \equiv q_y t / (T_h - T_c)$  is more useful. Thus, to compare the atomistic results with our BTE predictions we apply the conversion

$$\kappa_{yy} = \kappa_{yy,NEMD} \left( \frac{dT}{dy} \right) \left( \frac{t}{T_c - T_h} \right).$$

To obtain the BTE prediction, we first construct a simple analytical model describing phonon transport in graphite. Because graphite has highly anisotropic group velocities between the basal and cross-plane directions [38], the anisotropic Debye dispersion relation (Eq. (18)) for degenerate polarizations simplifies to a quasi-2D dispersion,  $\omega = v_{ab} k_{ab}$ . Molecular dynamics simulations rely upon classical rather than Bose-Einstein statistics, so to compare with the NEMD simulations we take the specific heat of each phonon mode to be  $C_k = k_B$ . As a first

approximation, we also assume that the scattering is gray ( $\tau_{\mathbf{k}} = \tau$  for all  $\mathbf{k}$ ). The benefit of these approximations is that the cross-plane thermal conductivity suppression function  $S_{yy} \equiv \kappa_{yy} / \kappa_{yy,bulk}$  becomes a universal function which only depends on the  $y$ -direction dimensionless mean free path  $\lambda_y \equiv \Lambda \sin \Psi / t$ , where  $\Lambda \equiv v_{ab} \tau$ . For example, under these approximations,  $S_{yy}$  does not depend on the size or shape of the first Brillouin zone.

We use  $\Lambda$  as the only fitting parameter to compare the BTE solutions with the NEMD simulations. As shown in Figure 3, the BTE model is in good agreement with the non-dimensionalized NEMD results for 24 different  $(\Psi, t)$  pairings using  $\Lambda = 103$  nm. We can assess the self-consistency of this fitting parameter by calculating the basal plane thermal conductivity using the quasi-2D expression  $\kappa = \frac{1}{2} C v_{ab} \Lambda$  and comparing with the bulk NEMD values of  $\kappa$ . To determine  $\kappa$ , we use the same input parameters for graphite as in a previous modeling study [38]. We calculate  $C = k_B \eta_{PUC}$ , where  $\eta_{PUC} = 5.56 * 10^{28} \text{ m}^{-3}$  is the primitive unit cell density, and we consider two degenerate polarizations with  $v_{ab} = 13,200 \text{ ms}^{-1}$ . This value for  $v_{ab}$  was obtained by averaging the basal-plane group velocities of the acoustic TA and TL1 polarizations from Ref. [38]. We note that we neglect the thermal conductivity contribution from the third acoustic (TL2) polarization and from the optical polarizations due to the smaller basal-plane group velocities and velocity anisotropy ratios. Finally, using our fit value of  $\Lambda$  gives  $\kappa = 1051 \text{ Wm}^{-1}\text{K}^{-1}$ , which is within 8% of the NEMD result  $\kappa = 1140 \pm 30 \text{ Wm}^{-1}\text{K}^{-1}$ . This good agreement indicates that the one-parameter anisotropic Debye model combined with the BTE solution accurately describes the phonon transport in NEMD atomistic simulations.

While the NEMD simulations can only be performed for relatively small thicknesses ( $t < 45$  nm here) due to computational constraints, the BTE solutions can be readily applied for a broader range of film thicknesses, as emphasized by the much larger span of the line as compared to the points in Fig. 3. The analytical BTE solution also provides insight into the size effects observed in the NEMD simulations: the most crucial parameter dictating the thermal conductivity suppression is the  $y$ -component of the mean free path, as also observed by Minnich for aligned thin films [4].

### C. Case study: In-plane off-diagonal transport in black phosphorus

The thermal properties of black phosphorus nanostructures have received recent attention [6,39–43] due to potential applications of black phosphorus or few-layer black phosphorene in nanoelectronics, optoelectronics, and thermoelectric energy conversion [26]. For example, the anisotropic in-plane electrical and optical properties of black phosphorus have been leveraged to demonstrate a polarization-sensitive broadband photodetector [44]. The thermal design of such black phosphorus devices will require an understanding of how the heat

transfer rates depend on the orientation of the temperature gradient with respect to the crystal structure.

Single-crystal black phosphorus has a larger thermal conductivity along the in-plane zigzag direction ( $\kappa_{ZZ}$ ) than in the orthogonal in-plane armchair direction ( $\kappa_{AC}$ ), with recently measured room temperature anisotropy ratios  $r \equiv \kappa_{ZZ} / \kappa_{AC}$  of  $r = 2.5 - 3$  [6,40–42]. Due to this in-plane anisotropy, a temperature gradient  $\frac{dT}{dx}$  imposed in the  $\hat{x}$  direction oriented at an angle  $\theta$  to the armchair direction induces a heat flow  $q_z = -\kappa_{zx} \frac{dT}{dx}$  in the orthogonal  $\hat{z}$  direction (see inset of Fig. 4). In the bulk regime, classic tensor rotation identities [45] show that  $\kappa_{zx} = \frac{1}{2}(\kappa_{ZZ} - \kappa_{AC})\sin(2\theta)$ . We will now show that our BTE solutions predict that this same simple identity applies for black phosphorus thin films even in the boundary scattering regime. We will then leverage previous first-principles calculations [6] to model  $\kappa_{zx}(t, \theta)$  of black phosphorus thin films.

We first consider in-plane thermal transport of aligned thin films (i.e.  $\Psi=0$  in Fig. 2). We consider a temperature difference imposed along  $\hat{x}$  and want to determine the heat flow in  $\hat{z}$  using the off-diagonal conductivity  $\kappa_{zx}$ . In the  $(x, y, z)$  coordinate system of Fig. 1 the off-diagonal conductivity  $\kappa_{zx}$  (Eq. (B3)) of an aligned film is

$$\kappa_{zx} = \frac{2}{V} \sum_{\lambda_{k,y} > 0} C_k v_{k,x} v_{k,z} \tau_k \left[ 1 - \lambda_{k,y} \left( 1 - \exp\left(-\frac{1}{\lambda_{k,y}}\right) \right) \right]. \quad (19)$$

If we instead choose to express the group velocity projections  $v_{k,x}$  and  $v_{k,z}$  in an alternate coordinate system  $(x', y, z')$  that is rotated about the  $y$  axis by an angle  $\theta$ , Eq. (19) becomes

$$\kappa_{zx} = \frac{2}{V} \sum_{\lambda_{k,y} > 0} C_k (v_{k,x'} \cos(\theta) + v_{k,z'} \sin(\theta)) (-v_{k,x'} \sin(\theta) + v_{k,z'} \cos(\theta)) \tau_k \left[ 1 - \lambda_{k,y} \left( 1 - \exp\left(-\frac{1}{\lambda_{k,y}}\right) \right) \right]. \quad (20)$$

Note that Eqs. (19) and (20) are simply different mathematical representations of the same physical quantity  $\kappa_{zx}$ . Multiplying out the different group velocity terms and rearranging, Eq. (20) can be written as

$$\begin{aligned}
\kappa_{zx} = & \cos(\theta)\sin(\theta) \left\{ \frac{2}{V} \sum_{\lambda_{k,y}>0} C_k v_{k,z'} v_{k,z'} \tau_k \left[ 1 - \lambda_{k,y} \left( 1 - \exp\left(-\frac{1}{\lambda_{k,y}}\right) \right) \right] \right\} \\
& - \cos(\theta)\sin(\theta) \left\{ \frac{2}{V} \sum_{\lambda_{k,y}>0} C_k v_{k,x'} v_{k,x'} \tau_k \left[ 1 - \lambda_{k,y} \left( 1 - \exp\left(-\frac{1}{\lambda_{k,y}}\right) \right) \right] \right\} \\
& + \left( \cos^2(\theta) - \sin^2(\theta) \right) \left\{ \frac{2}{V} \sum_{\lambda_{k,y}>0} C_k v_{k,x'} v_{k,z'} \tau_k \left[ 1 - \lambda_{k,y} \left( 1 - \exp\left(-\frac{1}{\lambda_{k,y}}\right) \right) \right] \right\}.
\end{aligned} \tag{21}$$

However, the terms from Eq. (21) in braces are identical to the BTE predictions of the conductivities  $\kappa_{z'z'}$ ,  $\kappa_{x'x'}$ , and  $\kappa_{x'z'}$  ( $= \kappa_{z'x'}$ ) that would be identified if temperature gradients and heat fluxes were imposed and measured in the  $(x', y, z')$  coordinate system. Therefore, our BTE solutions lead to the simple transformation identity

$$\kappa_{zx} = \frac{1}{2} (\kappa_{z'z'} - \kappa_{x'x'}) \sin(2\theta) + \kappa_{z'x'} \cos(2\theta), \tag{22}$$

where we have used the trigonometric identities  $\cos(\theta)\sin(\theta) = \sin(2\theta)/2$  and  $\cos^2(\theta) - \sin^2(\theta) = \cos(2\theta)$ . In Appendix C, we show that Eq. (22) also holds for the more general case of in-plane rotations of arbitrarily aligned films (i.e.  $\Psi \neq 0$  in Fig. 2).

Since Eq. (22) is the same relationship used in Fourier heat conduction [45], we have shown that the tensor rotation rules utilized in the bulk regime also apply for in-plane rotations in the thin film boundary scattering regime. This relationship indicates that it is not necessary to independently measure the in-plane thermal conductivity as a function of many directions  $\theta$ , even for a very thin film in which  $\kappa_{zx}$  will be dramatically reduced from its bulk value due to boundary scattering. Instead, only a maximum of three independent in-plane components need to be determined for a given  $t$ , and then Eq. (22) can be used to calculate  $\kappa_{zx}$  for any arbitrary  $\theta$ .

For our example of black phosphorus thin films with  $\Psi = 0$ , Eq. (22) further simplifies to  $\kappa_{zx} = \frac{1}{2} (\kappa_{ZZ} - \kappa_{AC}) \sin(2\theta)$ . Recently, Smith et al. [6] performed first-principles calculations to determine both the harmonic and anharmonic force constants required to find  $\kappa_{ZZ}$  and  $\kappa_{AC}$  of pure samples (no impurity scattering) without any fitting parameters. They also used the BTE solution for in-plane thin film boundary scattering in aligned materials [4] to calculate  $\kappa_{ZZ}(t)$  and  $\kappa_{AC}(t)$ . Here, we combine these first-principles predictions of  $\kappa_{ZZ}(t)$  and  $\kappa_{AC}(t)$  with the rotation transformation rule (Eq. (22)) to predict  $\kappa_{zx}(\theta, t)$  of black phosphorus thin films. Figure 4 shows the BTE predictions for  $\kappa_{zx}$  as a function of rotation angle for four different film thicknesses. Due to the large conductivity contrast between  $\kappa_{ZZ}(t)$  and  $\kappa_{AC}(t)$ , the off-

diagonal component  $\kappa_{zz}(t)$  can be as large as  $33 \text{ Wm}^{-1}\text{K}^{-1}$  for thick films ( $t=10 \text{ }\mu\text{m}$ ). Even for films as thin as  $t=10 \text{ nm}$ ,  $\kappa_{zz}$  can be as large as  $18 \text{ Wm}^{-1}\text{K}^{-1}$ , indicating that the thermal conductivity suppression from boundary scattering is relatively weak due to the phonon focusing along the in-plane directions.

These predictions for  $\kappa_{zz}(\theta, t)$  of black phosphorus thin films contain no free parameters and can be used to model the thermal performance of electronic and optoelectronics devices of any in-plane orientation, enabling improved thermal design of black phosphorus photodetectors, thermoelectric devices, or transistors. The tensor rotation relation derived here can also be readily applied to study thermal transport in other materials of recent interest with anisotropic in-plane thermal conductivities, including  $\text{ReS}_2$  [16] and black arsenic [46].

#### D. Discussion: Connection to recent experimental methods

The BTE solutions and Onsager proof presented here support recently developed experimental tools to measure the off-diagonal terms of the thermal conductivity tensor. Feser, Liu, and Cahill [47] developed new “beam offset” time-domain thermoreflectance (TDTR) measurement techniques to measure the full  $\mathbf{\kappa}$  tensor of thin films and bulk materials. The analysis in Ref. [47] implicitly assumed that the Onsager relation holds even for thin films, an assumption which our BTE solution shows to be rigorously justified. This beam offset method has recently been used to measure the diagonal components of the  $\mathbf{\kappa}$  tensor of bulk black phosphorus as a function of rotation angle  $\theta$  [41], and it should be straightforward to extend such measurements to a thin film sample to measure  $\kappa_{xz}(\theta, t)$  as suggested here in Fig. 4. In another class of measurements, Mishra *et al.* [48] used an electrothermal technique to measure the off-diagonal conductivity of arbitrarily aligned bulk mica. This off-diagonal measurement technique could plausibly be extended to thin films by adapting elements of the multiple-sensor “two-omega” method of Ramu and Bowers [49] or of the anisotropic thin film measurements of Ju, Kurabayashi, and Goodson [50]. Lastly, the zigzag and armchair thermal conductivities of black phosphorus nanoribbons have been measured using suspended heater/thermometer platforms [39] and suspended beams [6]. By measuring multiple samples of different alignments, these suspended device measurements could also be used to determine the in-plane off-diagonal component  $\kappa_{xz}$  and  $\kappa_{zx}$  of arbitrarily aligned nanostructures. Thus, several optical and/or electrothermal microscale thermal measurement techniques could be used to test the thin film Onsager relation predicted by the BTE theory, and the Onsager relation can likewise be used to simplify the analysis and measurement of systems containing anisotropic thin films.

#### IV. SUMMARY

In conclusion, we identified an Onsager reciprocity relation for ballistic phonon transport in thin films. This reciprocity relation states that the thermal conductivity tensor is symmetric from the diffusive regime through the thin film boundary scattering regime,

extending Onsager’s original reciprocity relation for anisotropic heat conduction to capture ballistic phonon transport effects. We illustrated the boundary scattering suppression and reciprocity relation using a simple model for anisotropic materials, compared the BTE solutions to atomistic simulations [35] of arbitrarily aligned graphite, and modeled thin-film size effects on the off-diagonal thermal conductivity of rotated black phosphorus using previous first-principles calculations of only the principal components [6]. This thermal conductivity reciprocity relation reduces the number of independent measurements that are required to fully characterize thermal transport in anisotropic thin films.

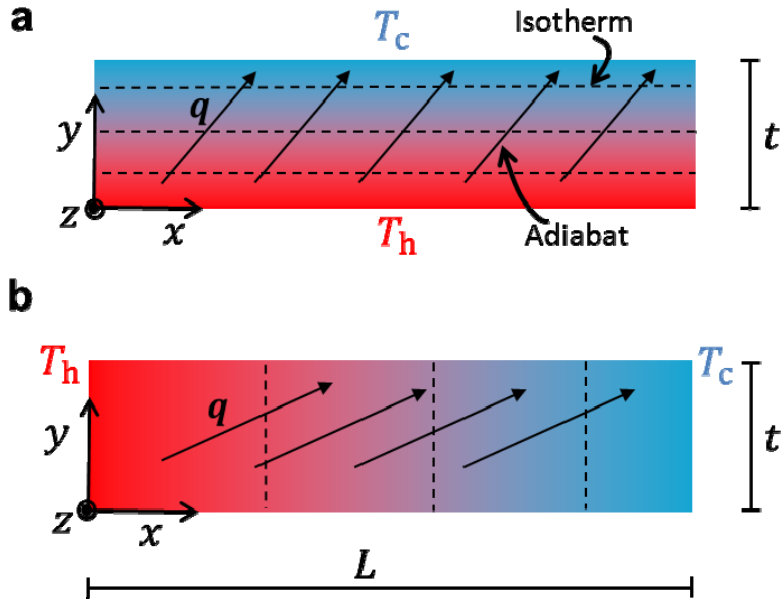


FIG. 1. Schematic of anisotropic heat transfer in thin films due to (a) cross-plane and (b) in-plane temperature differences ( $T_h - T_c$ ). In arbitrarily aligned anisotropic materials, the heat flux  $\mathbf{q}$  is not necessarily antiparallel to the temperature gradient  $\nabla T$ , as represented by non-orthogonal adiabats and isotherms in (a,b) and mathematically described by off-diagonal components of the thermal conductivity tensor  $\kappa$ . We use Boltzmann transport equation solutions to prove that  $\kappa$  remains symmetric from the bulk through the thin film boundary scattering regime: for example, we show that the off-diagonal thermal conductivities  $\kappa_{xy}$  and  $\kappa_{yx}$  are equal. Here,  $\kappa_{xy}$  is the ratio of the heat flow in  $x$  per unit depth  $Q'_x$  to the imposed temperature difference in  $y$  (as in (a)), and  $\kappa_{yx}$  is the ratio of the heat flow in  $y$  per unit depth  $Q'_y$  due to the temperature difference in  $x$  (as in (b)).

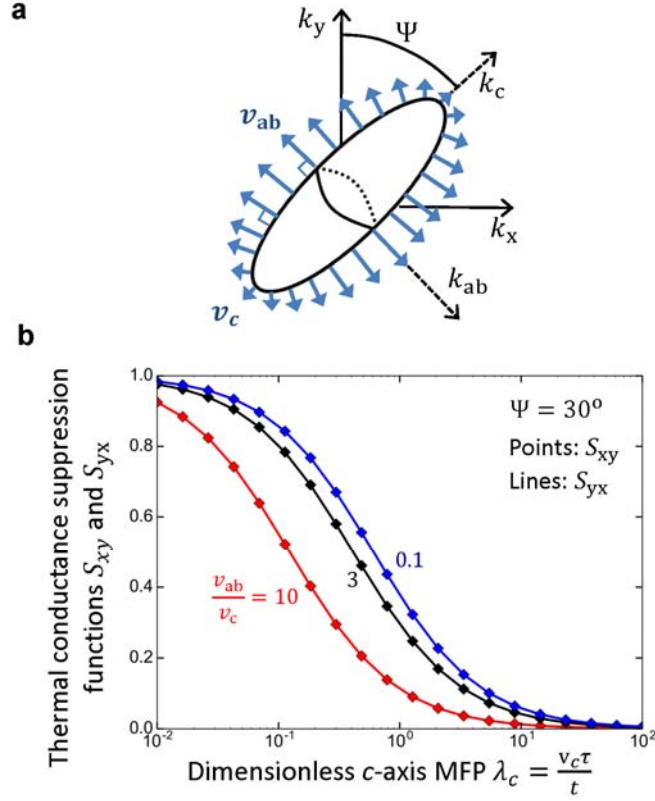


FIG. 2. A numerical demonstration of the reciprocity relation  $\kappa_{xy} = \kappa_{yx}$ . (a) Reciprocal-space schematic of the iso-frequency ellipsoid for a material with an anisotropic Debye dispersion relation (Eq. (18)). The  $\hat{c}$  axis of the material is tilted by an angle  $\Psi$  with respect to the  $\hat{y}$  direction of the film. For simplicity we consider a constant relaxation time  $\tau$ , high temperatures, and a spherical first Brillouin zone. (b) According to the reciprocity relation  $\kappa_{xy} = \kappa_{yx}$  (Eq. (17)), the off-diagonal thermal conductivity suppression functions  $S_{ij} = \kappa_{ij} / \kappa_{ij,bulk}$  are supposed to be equal ( $S_{xy} = S_{yx}$ ) for all values of the dimensionless mean free path  $\lambda_c$  from the diffusive ( $\lambda_c \ll 1$ ) through the boundary scattering ( $\lambda_c \gg 1$ ) regimes. Here this  $S_{xy} = S_{yx}$  equality is verified numerically using Eqs. (13) and (14) for the particular case of  $\Psi = 30^\circ$  and three values of the group velocity anisotropy ratio  $v_{ab} / v_c$ .

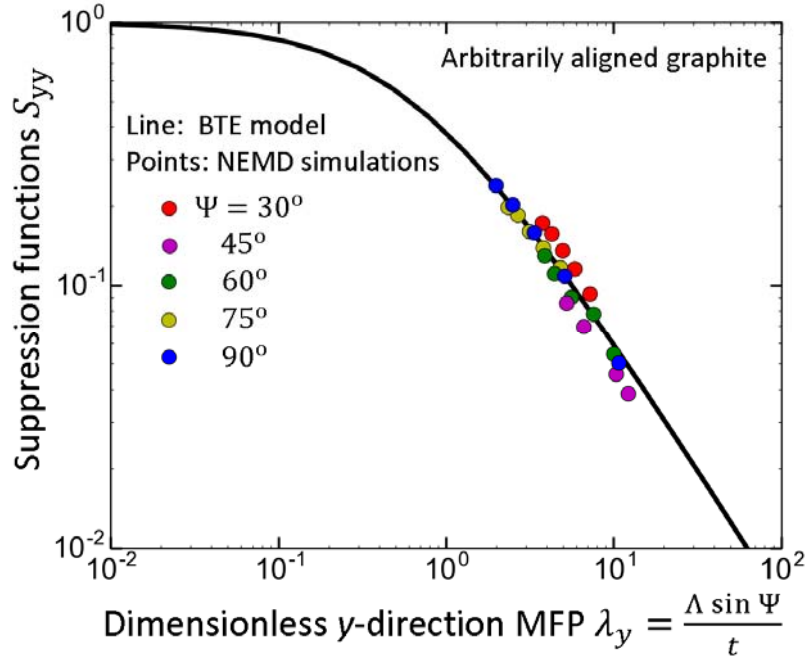


FIG 3. Comparing the analytical BTE solutions to non-equilibrium molecular dynamics (NEMD) simulations of arbitrarily aligned graphite [35]. The NEMD simulations were performed for 24 combinations of basal plane alignment angles  $\Psi$  (see Fig 2) and film thickness  $t$ . The BTE model for highly anisotropic layered materials agrees well with the numerical results using a gray mean free path  $\Lambda = 103$  nm.

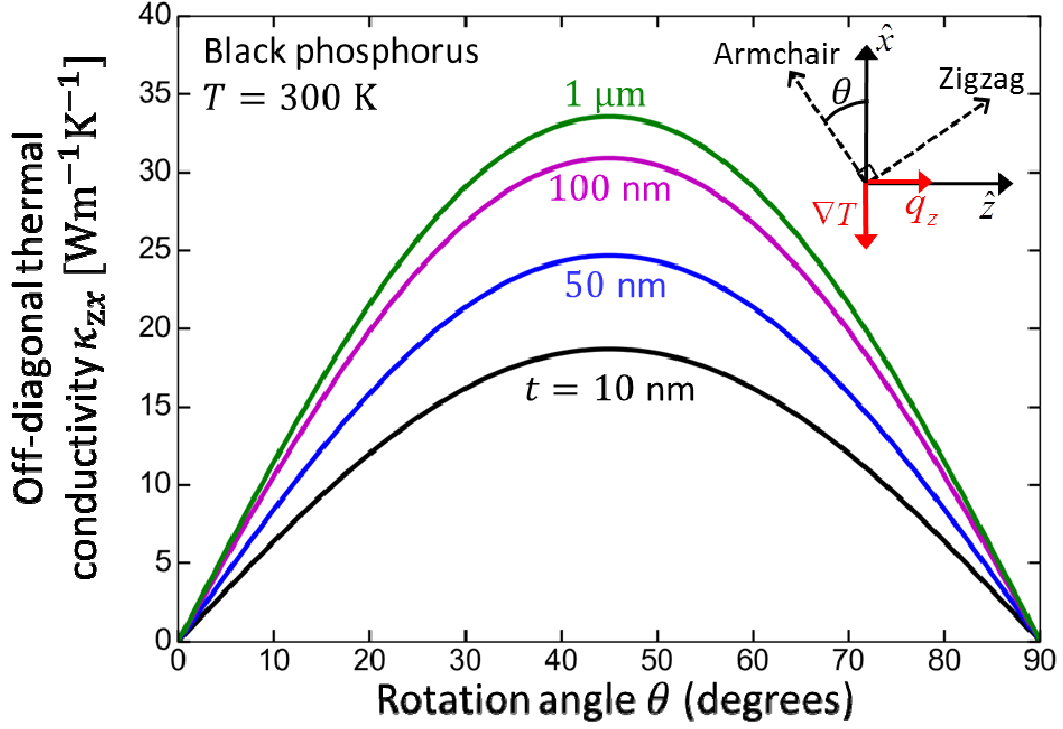


FIG 4. Thin-film boundary scattering reduces the off-diagonal in-plane thermal conductivity  $\kappa_{zx}$  of black phosphorus. The BTE solutions show that  $\kappa_{zx}$  can be determined for a given in-plane temperature gradient rotation angle  $\theta$  using simple tensor transformation identities, even in the boundary scattering regime. We use recent first-principles calculations [6] of thickness-dependent  $\kappa$  along the zigzag and armchair directions at room temperature to calculate  $\kappa_{zx}(\theta, t)$  for aligned black phosphorus thin films ( $\Psi = 0$ ).

## Appendix A: BTE solution for in-plane temperature differences

Here, we detail the intermediate steps of the derivation for the BTE solution for in-plane temperature differences. Using an integrating factor, we obtain the formal solution to the BTE (Eq. (9)) as

$$j_{\mathbf{k}}^+(\eta) = j_{\mathbf{k},0}^+ \exp\left(-\frac{\eta}{\lambda_{\mathbf{k},y}}\right) + \int_{\eta'=0}^{\eta} [\lambda_{\mathbf{k},x} + \Delta T_x(\eta')] \exp\left(-\frac{\eta-\eta'}{\lambda_{\mathbf{k},y}}\right) \frac{d\eta'}{\lambda_{\mathbf{k},y}} \quad (\text{A1})$$

$$j_{\mathbf{k}}^-(\eta) = j_{\mathbf{k},1}^- \exp\left(\frac{1-\eta}{\lambda_{\mathbf{k},y}}\right) - \int_{\eta'=\eta}^1 [\lambda_{\mathbf{k},x} + \Delta T_x(\eta')] \exp\left(-\frac{\eta-\eta'}{\lambda_{\mathbf{k},y}}\right) \frac{d\eta'}{\lambda_{\mathbf{k},y}}. \quad (\text{A2})$$

Here  $j_{\mathbf{k}}^+(\eta)$  is the distribution function for phonons travelling upward ( $\lambda_{\mathbf{k},y} > 0$ ), and  $j_{\mathbf{k}}^-(\eta)$  is the distribution function for phonons travelling downward ( $\lambda_{\mathbf{k},y} < 0$ ). We fix the integration constants  $j_{\mathbf{k},0}^+$  and  $j_{\mathbf{k},1}^-$  using the boundary conditions at the walls. Since the walls are treated as black emitters,  $f_{\mathbf{k}} = f_{\mathbf{k},0}(T_{r,x})$  for all phonons leaving the walls. Applying this boundary condition to Eqs. (A1) and (A2) yields  $j_{\mathbf{k},0}^+ = j_{\mathbf{k},1}^- = 0$ .

Now we implement the energy conservation requirement, which is

$$\Delta T_x(\eta) = \left( \sum_{\mathbf{k}} \frac{C_{\mathbf{k}}}{\tau_{\mathbf{k}}} \right)^{-1} \left( \sum_{\mathbf{k}} \frac{C_{\mathbf{k}}}{\tau_{\mathbf{k}}} j_{\mathbf{k}} \right). \quad (\text{A3})$$

Plugging Eqs.(A1) and (A2) into Eq. (A3), we obtain

$$\Delta T_x(\eta) = \left( \sum_{\mathbf{k}} \frac{C_{\mathbf{k}}}{\tau_{\mathbf{k}}} \right)^{-1} \left\{ \begin{array}{l} \left[ \sum_{\lambda_{\mathbf{k},y}>0} \frac{C_{\mathbf{k}}}{\tau_{\mathbf{k}}} \int_{\eta'=0}^{\eta} [\lambda_{\mathbf{k},x} + \Delta T_x(\eta')] \exp\left(-\frac{\eta-\eta'}{\lambda_{\mathbf{k},y}}\right) \frac{d\eta'}{\lambda_{\mathbf{k},y}} \right] \\ - \left[ \sum_{\lambda_{\mathbf{k},y}<0} \frac{C_{\mathbf{k}}}{\tau_{\mathbf{k}}} \int_{\eta'=\eta}^1 [\lambda_{\mathbf{k},x} + \Delta T_x(\eta')] \exp\left(-\frac{\eta-\eta'}{\lambda_{\mathbf{k},y}}\right) \frac{d\eta'}{\lambda_{\mathbf{k},y}} \right] \end{array} \right\}. \quad (\text{A4})$$

Using the inversion symmetries of the dispersion and scattering, we change the summation over  $\lambda_{\mathbf{k},y} < 0$  in Eq. (A4) to an equivalent summation over  $\lambda_{\mathbf{k},y} > 0$  as

$$\Delta T_x(\eta) = \left( \sum_{\mathbf{k}} \frac{C_{\mathbf{k}}}{\tau_{\mathbf{k}}} \right)^{-1} \left\{ \begin{aligned} & \left[ \sum_{\lambda_{\mathbf{k},y} > 0} \frac{C_{\mathbf{k}}}{\tau_{\mathbf{k}}} \int_{\eta'=0}^{\eta} [\lambda_{\mathbf{k},x} + \Delta T_x(\eta')] \exp\left(-\frac{\eta-\eta'}{\lambda_{\mathbf{k},y}}\right) \frac{d\eta'}{\lambda_{\mathbf{k},y}} \right] \\ & + \left[ \sum_{\lambda_{\mathbf{k},y} > 0} \frac{C_{\mathbf{k}}}{\tau_{\mathbf{k}}} \int_{\eta'=\eta}^1 [-\lambda_{\mathbf{k},x} + \Delta T_x(\eta')] \exp\left(\frac{\eta-\eta'}{\lambda_{\mathbf{k},y}}\right) \frac{d\eta'}{\lambda_{\mathbf{k},y}} \right] \end{aligned} \right\}. \quad (\text{A5})$$

Combining the summations in Eq. (A5) and rearranging,

$$\Delta T_x(\eta) = \left( \sum_{\mathbf{k}} \frac{C_{\mathbf{k}}}{\tau_{\mathbf{k}}} \right)^{-1} \sum_{\lambda_{\mathbf{k},y} > 0} \frac{C_{\mathbf{k}}}{\tau_{\mathbf{k}}} \lambda_{\mathbf{k},x} \left( \begin{aligned} & \left( \int_{\eta'=0}^{\eta} \exp\left(-\frac{\eta-\eta'}{\lambda_{\mathbf{k},y}}\right) \frac{d\eta'}{\lambda_{\mathbf{k},y}} - \int_{\eta'=\eta}^1 \exp\left(\frac{\eta-\eta'}{\lambda_{\mathbf{k},y}}\right) \frac{d\eta'}{\lambda_{\mathbf{k},y}} \right) \\ & + \int_{\eta'=0}^1 \Delta T_x(\eta') \exp\left(\frac{|\eta-\eta'|}{\lambda_{\mathbf{k},y}}\right) \frac{d\eta'}{\lambda_{\mathbf{k},y} \lambda_{\mathbf{k},x}} \end{aligned} \right). \quad (\text{A6})$$

After performing the first two integrals in Eq. (A6) analytically, we obtain Eq. (10).

### Appendix B: Proof of the in-plane reciprocity relation $\kappa_{xz} = \kappa_{zx}$

We begin by using our in-plane BTE solution to find  $\kappa_{zx} \equiv Q_z' / (T_h - T_c)$ , where  $Q_z'$  is the heat flow in the in-plane  $\hat{z}$  direction divided by  $t$ . Our solution proceeds analogously to the derivation of the reciprocity relation in the main text (Eq. (17)). Substituting our definition of  $j_{\mathbf{k}}$  into Eq. (2), integrating over the film thickness, and dividing by  $(T_h - T_c)$ , we obtain

$$\kappa_{zx} = \frac{L}{V} \sum_{\mathbf{k}} C_{\mathbf{k}} \nu_{\mathbf{k},z} \int_0^1 j_{\mathbf{k}} d\eta. \quad (\text{B1})$$

We integrate the in-plane BTE (Eq. (9)) from  $\eta = 0$  to 1 to obtain an expression for  $\int_0^1 j_{\mathbf{k}} d\eta$ , and then determine  $j_{\mathbf{k}}(0)$  and  $j_{\mathbf{k}}(1)$  using the integral form of the BTE. Substituting into Eq. (B1), we obtain

$$\begin{aligned} \kappa_{zx} = \frac{L}{V} \sum_{\lambda_{\mathbf{k},y} > 0} C_{\mathbf{k}} \nu_{\mathbf{k},z} \left\{ \left( \lambda_{\mathbf{k},x} - \lambda_{\mathbf{k},x} \lambda_{\mathbf{k},y} \left( 1 - \exp\left(-\frac{1}{\lambda_{\mathbf{k},y}}\right) \right) \right) - \int_{\eta'=0}^1 \Delta T_x(\eta') \exp\left(-\frac{1-\eta'}{\lambda_{\mathbf{k},y}}\right) d\eta' + \int_0^1 \Delta T_x d\eta \right\} \\ + \frac{L}{V} \sum_{\lambda_{\mathbf{k},y} < 0} C_{\mathbf{k}} \nu_{\mathbf{k},z} \left\{ \left( \lambda_{\mathbf{k},x} - \lambda_{\mathbf{k},x} \lambda_{\mathbf{k},y} \left( \exp\left(\frac{1}{\lambda_{\mathbf{k},y}}\right) - 1 \right) \right) - \int_{\eta'=0}^1 \Delta T_x(\eta') \exp\left(\frac{\eta'}{\lambda_{\mathbf{k},y}}\right) d\eta' + \int_0^1 \Delta T_x d\eta \right\}. \end{aligned} \quad (\text{B2})$$

Using the symmetries of the dispersion relation to convert the summation over  $\lambda_{\mathbf{k},y} < 0$  to an equivalent summation over  $\lambda_{\mathbf{k},y} > 0$ , we simplify Eq. (B2) as

$$\begin{aligned} \kappa_{zx} &= \kappa_{zx,bulk} - \frac{2}{V} \sum_{\lambda_{\mathbf{k},y} > 0} \kappa_{\mathbf{k},xz} \lambda_{\mathbf{k},y} \left( 1 - \exp\left(-\frac{1}{\lambda_{\mathbf{k},y}}\right) \right) \\ &\quad - \frac{1}{V} \sum_{\lambda_{\mathbf{k},y} > 0} \kappa_{\mathbf{k},xz} \int_{\eta'=0}^1 \Delta T_x(\eta') \left( \exp\left(-\frac{1-\eta'}{\lambda_{\mathbf{k},y}}\right) - \exp\left(-\frac{\eta'}{\lambda_{\mathbf{k},y}}\right) \right) \frac{d\eta'}{\lambda_{\mathbf{k},x}}, \end{aligned} \quad (\text{B3})$$

where  $\kappa_{\mathbf{k},xz} \equiv C_{\mathbf{k}} v_{\mathbf{k},x} v_{\mathbf{k},z} \tau_{\mathbf{k}}$  and  $\kappa_{zx,bulk} = \frac{1}{V} \sum_{\mathbf{k}} \kappa_{\mathbf{k},xz}$ .

As previously noted in Section II.C, the designation of the in-plane direction  $\hat{x}$  was arbitrary. Therefore, to assist in identifying the thermal conductivity component  $\kappa_{xz}$  we can write down the deviational temperature profile  $\Delta T_z(\eta)$  due to an imposed temperature difference  $(T_h - T_c)$  in  $\hat{z}$  by direct analogy with Eq. (10) as

$$\Delta T_z(\eta) = \left( \sum_{\mathbf{k}} \frac{C_{\mathbf{k}}}{\tau_{\mathbf{k}}} \right)^{-1} \sum_{\lambda_{\mathbf{k},z} > 0} \frac{C_{\mathbf{k}}}{\tau_{\mathbf{k}}} \lambda_{\mathbf{k},z} \left[ \exp\left(-\frac{1-\eta}{\lambda_{\mathbf{k},y}}\right) - \exp\left(-\frac{\eta}{\lambda_{\mathbf{k},y}}\right) + \int_{\eta'=0}^1 \Delta T_z(\eta') \exp\left(-\frac{|\eta-\eta'|}{\lambda_{\mathbf{k},y}}\right) \frac{d\eta'}{\lambda_{\mathbf{k},y} \lambda_{\mathbf{k},z}} \right]. \quad (\text{B4})$$

Here,  $\lambda_{\mathbf{k},z} = v_{\mathbf{k},z} \tau_{\mathbf{k}} / w$ , where  $w$  is the width of the sample in  $\hat{z}$ . By following the same procedure described in the development of Eqs. (B1)-(B3), we find

$$\begin{aligned} \kappa_{xz} &= \kappa_{xz,bulk} - \frac{2}{V} \sum_{\lambda_{\mathbf{k},y} > 0} \kappa_{\mathbf{k},xz} \lambda_{\mathbf{k},y} \left( 1 - \exp\left(-\frac{1}{\lambda_{\mathbf{k},y}}\right) \right) \\ &\quad - \frac{1}{V} \sum_{\lambda_{\mathbf{k},y} > 0} \kappa_{\mathbf{k},xz} \int_{\eta'=0}^1 \Delta T_z(\eta') \left( \exp\left(-\frac{1-\eta'}{\lambda_{\mathbf{k},y}}\right) - \exp\left(-\frac{\eta'}{\lambda_{\mathbf{k},y}}\right) \right) \frac{d\eta'}{\lambda_{\mathbf{k},z}}. \end{aligned} \quad (\text{B5})$$

Subtracting Eq. (B5) from Eq. (B3) and rearranging,

$$\begin{aligned} \kappa_{zx} - \kappa_{xz} &= -\frac{LW}{V} \int_{\eta'=0}^1 \Delta T_x(\eta') \left\{ \sum_{\lambda_{\mathbf{k},y} > 0} \frac{C_{\mathbf{k}}}{\tau_{\mathbf{k}}} \lambda_{\mathbf{k},z} \left( \exp\left(-\frac{1-\eta'}{\lambda_{\mathbf{k},y}}\right) - \exp\left(-\frac{\eta'}{\lambda_{\mathbf{k},y}}\right) \right) \right\} d\eta' \\ &\quad + \frac{LW}{V} \int_{\eta'=0}^1 \Delta T_z(\eta') \left\{ \sum_{\lambda_{\mathbf{k},y} > 0} \frac{C_{\mathbf{k}}}{\tau_{\mathbf{k}}} \lambda_{\mathbf{k},x} \left( \exp\left(-\frac{1-\eta'}{\lambda_{\mathbf{k},y}}\right) - \exp\left(-\frac{\eta'}{\lambda_{\mathbf{k},y}}\right) \right) \right\} d\eta'. \end{aligned} \quad (\text{B6})$$

Using the integral temperature solutions of the BTE (Eqs. (10) and (B4)) to simplify Eq. (B6), we find

$$\kappa_{zx} - \kappa_{xz} = \frac{LW}{V} \sum_{\lambda_{k,y} > 0} \frac{C_k}{\tau_k} \int_{\eta=0}^1 \int_{\eta'=0}^1 \exp\left(-\frac{|\eta-\eta'|}{\lambda_{k,y}}\right) (\Delta T_x(\eta) \Delta T_z(\eta') - \Delta T_x(\eta') \Delta T_z(\eta)) \frac{d\eta'}{\lambda_{k,y}} d\eta. \quad (\text{B7})$$

Finally, using the same rationale leading to Eq. (17), the anti-symmetric integrand with equivalent limits of integration for Eq. (B7) implies that  $\kappa_{zx} - \kappa_{xz} = 0$ . Therefore, the BTE solution shows that  $\kappa_{zx} = \kappa_{xz}$ .

### Appendix C: In-plane rotations of arbitrarily aligned thin films

We now consider the general scenario of in-plane transport in arbitrarily aligned films (i.e.  $\Psi \neq 0^\circ$  in Fig. 2). A temperature gradient  $-(T_h - T_c)/L_x$  imposed along  $\hat{x}$  induces a cross-plane deviational temperature profile  $\Delta T_x(\eta)$ , which is found by solving the integral form of the BTE (Eq. (10)). Rearranging Eq. (10) to separate  $\Delta T_x(\eta)$  from terms that depend on  $v_{k,x}$  gives

$$\begin{aligned} & \sum_{\lambda_{k,y} > 0} \frac{C_k}{\tau_k} \left( 2\Delta T_x(\eta) - \int_{\eta'=0}^1 \Delta T_x(\eta') \exp\left(-\frac{|\eta-\eta'|}{\lambda_{k,y}}\right) \frac{d\eta'}{\lambda_{k,y}} \right) \\ &= \sum_{\lambda_{k,y} > 0} \frac{C_k v_{k,x}}{L_x} \left[ \exp\left(-\frac{1-\eta}{\lambda_{k,y}}\right) - \exp\left(-\frac{\eta}{\lambda_{k,y}}\right) \right]. \end{aligned} \quad (\text{C1})$$

Due to the arbitrary choice of in-plane direction  $\hat{x}$ , analogous expressions for the deviational temperature profiles  $\Delta T_{x'}(\eta)$  ( $\Delta T_{z'}(\eta)$ ) due to a temperature gradient  $-(T_h - T_c)/L_{x'}$  ( $-(T_h - T_c)/L_{z'}$ ) imposed along in-plane directions  $x'$  ( $z'$ ) can be immediately written down by simply changing the subscript  $x$  to  $x'$  ( $z'$ ) in Eq. (C1).

If we choose to express Eq. (C1) for  $\Delta T_x(\eta)$  in the rotated  $(x', y, z')$  coordinate system, we can use the relation  $v_{k,x} = v_{k,x'} \cos(\theta) + v_{k,z'} \sin(\theta)$  to write Eq. (C1) as

$$\begin{aligned} & \sum_{\lambda_{k,y} > 0} \frac{C_k}{\tau_k} \left( 2\Delta T_x(\eta) - \int_{\eta'=0}^1 \Delta T_x(\eta') \exp\left(-\frac{|\eta-\eta'|}{\lambda_{k,y}}\right) \frac{d\eta'}{\lambda_{k,y}} \right) \\ &= \cos(\theta) \frac{L_{x'}}{L_x} \sum_{\lambda_{k,y} > 0} \frac{C_k v_{k,x'}}{L_{x'}} \left[ \exp\left(-\frac{1-\eta}{\lambda_{k,y}}\right) - \exp\left(-\frac{\eta}{\lambda_{k,y}}\right) \right] \\ &+ \sin(\theta) \frac{L_{z'}}{L_x} \sum_{\lambda_{k,y} > 0} \frac{C_k v_{k,z'}}{L_{z'}} \left[ \exp\left(-\frac{1-\eta}{\lambda_{k,y}}\right) - \exp\left(-\frac{\eta}{\lambda_{k,y}}\right) \right]. \end{aligned} \quad (\text{C2})$$

The two terms on the RHS of Eq. (C2) also appear in the RHS of integral equation solutions for  $\Delta T_{x'}(\eta)$  and  $\Delta T_{z'}(\eta)$  that are analogous to Eq. (C1). After substituting these integral equations, Eq. (C2) can be written as

$$\begin{aligned} & \sum_{\lambda_{k,y}>0} \frac{C_k}{\tau_k} \left( 2\Delta T_x(\eta) - \int_{\eta'=0}^1 \Delta T_x(\eta') \exp\left(-\frac{|\eta-\eta'|}{\lambda_{k,y}}\right) \frac{d\eta'}{\lambda_{k,y}} \right) \\ &= \cos(\theta) \frac{L_{x'}}{L_x} \sum_{\lambda_{k,y}>0} \frac{C_k}{\tau_k} \left( 2\Delta T_{x'}(\eta) - \int_{\eta'=0}^1 \Delta T_{x'}(\eta') \exp\left(-\frac{|\eta-\eta'|}{\lambda_{k,y}}\right) \frac{d\eta'}{\lambda_{k,y}} \right) \\ &+ \sin(\theta) \frac{L_{z'}}{L_x} \sum_{\lambda_{k,y}>0} \frac{C_k}{\tau_k} \left( 2\Delta T_{z'}(\eta) - \int_{\eta'=0}^1 \Delta T_{z'}(\eta') \exp\left(-\frac{|\eta-\eta'|}{\lambda_{k,y}}\right) \frac{d\eta'}{\lambda_{k,y}} \right) \end{aligned} \quad (C3)$$

By substituting into Eq. (C3), it can be shown that the deviational temperature profile due to a temperature gradient along  $\hat{x}$  is  $\Delta T_x(\eta) = (L_{x'}\Delta T_{x'}(\eta)\cos(\theta) + L_{z'}\Delta T_{z'}(\eta)\sin(\theta)) / L_x$ . We note here that our final results will not depend on the macroscopic dimensions  $L_{x'}$ ,  $L_{z'}$ , or  $L_x$ .

For arbitrarily aligned films, the off-diagonal thermal conductivity  $\kappa_{zx}$  is (Eq. (B3))

$$\kappa_{zx} = \frac{2}{V} \sum_{\lambda_{k,y}>0} \kappa_{k,xz} \left[ 1 - \lambda_{k,y} \left( 1 - \exp\left(-\frac{1}{\lambda_{k,y}}\right) \right) - \int_{\eta'=0}^1 \Delta T_x(\eta') \left( \exp\left(-\frac{1-\eta'}{\lambda_{k,y}}\right) - \exp\left(-\frac{\eta'}{\lambda_{k,y}}\right) \right) \frac{d\eta'}{2\lambda_{k,x}} \right]. \quad (C4)$$

Expressing  $v_{k,x}$ ,  $v_{k,z}$ , and  $\Delta T_x(\eta)$  in the rotated  $(x', y, z')$  coordinate system, we see that

$$\begin{aligned} \kappa_{zx} &= \frac{\sin(2\theta)}{2} \left\{ \frac{2}{V} \sum_{\lambda_{k,y}>0} \kappa_{k,z'z'} \left[ 1 - \lambda_{k,y} \left( 1 - \exp\left(-\frac{1}{\lambda_{k,y}}\right) \right) - \int_{\eta'=0}^1 \Delta T_{z'}(\eta') \left( \exp\left(-\frac{1-\eta'}{\lambda_{k,y}}\right) - \exp\left(-\frac{\eta'}{\lambda_{k,y}}\right) \right) \frac{d\eta'}{2\lambda_{k,z'}} \right] \right\} \\ &- \frac{\sin(2\theta)}{2} \left\{ \frac{2}{V} \sum_{\lambda_{k,y}>0} \kappa_{k,x'x'} \left[ 1 - \lambda_{k,y} \left( 1 - \exp\left(-\frac{1}{\lambda_{k,y}}\right) \right) - \int_{\eta'=0}^1 \Delta T_{x'}(\eta') \left( \exp\left(-\frac{1-\eta'}{\lambda_{k,y}}\right) - \exp\left(-\frac{\eta'}{\lambda_{k,y}}\right) \right) \frac{d\eta'}{2\lambda_{k,x'}} \right] \right\} \\ &+ \cos^2(\theta) \left\{ \frac{2}{V} \sum_{\lambda_{k,y}>0} \kappa_{k,x'z'} \left[ 1 - \lambda_{k,y} \left( 1 - \exp\left(-\frac{1}{\lambda_{k,y}}\right) \right) - \int_{\eta'=0}^1 \Delta T_{x'}(\eta') \left( \exp\left(-\frac{1-\eta'}{\lambda_{k,y}}\right) - \exp\left(-\frac{\eta'}{\lambda_{k,y}}\right) \right) \frac{d\eta'}{2\lambda_{k,x'}} \right] \right\} \\ &- \sin^2(\theta) \left\{ \frac{2}{V} \sum_{\lambda_{k,y}>0} \kappa_{k,z'x'} \left[ 1 - \lambda_{k,y} \left( 1 - \exp\left(-\frac{1}{\lambda_{k,y}}\right) \right) - \int_{\eta'=0}^1 \Delta T_{z'}(\eta') \left( \exp\left(-\frac{1-\eta'}{\lambda_{k,y}}\right) - \exp\left(-\frac{\eta'}{\lambda_{k,y}}\right) \right) \frac{d\eta'}{2\lambda_{k,z'}} \right] \right\}. \end{aligned} \quad (C5)$$

The first two terms in braces on the RHS of Eq. (C5) are simply  $\kappa_{z'z'}$  and  $\kappa_{x'x'}$ , while the last two terms in braces are  $\kappa_{z'x'}$  and  $\kappa_{x'z'}$ . Using the Onsager relation  $\kappa_{z'x'} = \kappa_{x'z'}$  derived in Appendix B,

Eq. (C5) can be finally written as  $\kappa_{zx} = \frac{1}{2}(\kappa_{z'z'} - \kappa_{x'x'})\sin(2\theta) + \kappa_{x'z'}\cos(2\theta)$ . Thus, we have

proved that the same tensor rotation rules utilized in the bulk regime also apply for in-plane rotations in the thin film boundary scattering regime.

**Acknowledgements:** G.W. and A.D.P. acknowledge support by the NSF GRFP under Grant No. 1106400. The authors thank Chenhan Liu for helpful discussions and for providing the NEMD data.

## References:

- [1] K. Fuchs and N. F. Mott, *Math. Proc. Cambridge Philos. Soc.* **34**, 100 (1938).
- [2] E. H. Sondheimer, *Adv. Phys.* **1**, 1 (1952).
- [3] A. Majumdar, *J. Heat Transfer* **115**, 7 (1993).
- [4] A. J. Minnich, *Appl. Phys. Lett.* **107**, 183106 (2015).
- [5] B. Vermeersch, J. Carrete, and N. Mingo, *Appl. Phys. Lett.* **108**, 193104 (2016).
- [6] B. Smith, B. Vermeersch, J. Carrete, E. Ou, J. Kim, N. Mingo, D. Akinwande, and L. Shi, *Adv. Mater.* **29**, 1603756 (2017).
- [7] A. M. Marconnet, M. Asheghi, and K. E. Goodson, *J. Heat Transfer* **135**, 061601 (2013).
- [8] Z. Aksamija and I. Knezevic, *Phys. Rev. B* **82**, 045319 (2010).
- [9] S. Neogi, J. S. Reparaz, L. F. C. Pereira, B. Graczykowski, M. R. Wagner, M. Sledzinska, A. Shchepetov, M. Prunnila, J. Ahopelto, C. M. Sontomayor-Torres, and D. Donadio, *ACS Nano* **9**, 3820 (2015).
- [10] P. Jiang, L. Lindsay, X. Huang, and Y. K. Koh, *Phys. Rev. B* **97**, 195308 (2018).
- [11] W. Prellier, M. P. Singh, and P. Murugavel, *J. Phys. Condens. Matter* **17**, R803 (2005).
- [12] M. Kang, K. Cho, S. Oh, J. Kim, C. Kang, S. Nahm, and S.-J. Yoon, *Appl. Phys. Lett.* **98**, 142102 (2011).
- [13] D. M. Berg, R. Djemour, L. Gütay, G. Zoppi, S. Siebentritt, and P. J. Dale, *Thin Solid Films* **520**, 6291 (2012).
- [14] D. M. Hausmann and R. G. Gordon, *J. Cryst. Growth* **249**, 251 (2003).
- [15] D. Ruzmetov and S. Ramanathan, in *Thin Film Met. Oxides*, edited by S. Ramanathan (Springer US, Boston, MA, 2010), pp. 51–94.
- [16] H. Jang, C. R. Ryder, J. D. Wood, M. C. Hersam, and D. G. Cahill, *Adv. Mater.* **29**, 1700650 (2017).
- [17] M. D. Santia, N. Tandon, and J. D. Albrecht, *Appl. Phys. Lett.* **107**, 041907 (2015).
- [18] Z. Guo, A. Verma, X. Wu, F. Sun, A. Hickman, T. Masui, A. Kuramata, M. Higashiwaki, D. Jena, and T. Luo, *Appl. Phys. Lett.* **106**, 111909 (2015).
- [19] J. P. Singh and R. K. Bedi, *J. Appl. Phys.* **68**, 2776 (1990).
- [20] O. Ambacher, *J. Phys. D: Appl. Phys.* **31**, 2653 (1998).
- [21] F. Scholz, *Semicond. Sci. Technol.* **27**, 024002 (2012).
- [22] H. N. Lee, D. Hesse, H. Nyung, and D. Hesse, *Appl. Phys. Lett.* **80**, 1040 (2002).
- [23] L. R. Testardi, *Appl. Phys. Lett.* **64**, 2347 (1994).
- [24] S. Lee, K. Hippalgaonkar, F. Yang, J. Hong, C. Ko, J. Suh, K. Liu, K. Wang, J. J. Urban, X. Zhang, C. Dames, S. A. Hartnoll, O. Delaire, and J. Wu, *Science* **355**, 371 (2016).
- [25] D.-W. Oh, C. Ko, S. Ramanathan, and D. G. Cahill, *Appl. Phys. Lett.* **96**, 151906 (2010).
- [26] X. Ling, H. Wang, S. Huang, F. Xia, and M. S. Dresselhaus, *Proc. Natl. Acad. Sci.* **112**, 4523 (2015).
- [27] L.-D. Zhao, S.-H. Lo, Y. Zhang, H. Sun, G. Tan, C. Uher, C. Wolverton, V. P. Dravid, and M. G. Kanatzidis, *Nature* **508**, 373 (2014).
- [28] X. Yan, B. Poudel, Y. Ma, W. S. Liu, G. Joshi, H. Wang, Y. Lan, D. Wang, G. Chen, and Z. F. Ren, *Nano Lett.* **10**, 3373 (2010).
- [29] R. Fei, A. Faghaninia, R. Soklaski, J. A. Yan, C. Lo, and L. Yang, *Nano Lett.* **14**, 6393 (2014).
- [30] Y. Tang, B. Cui, C. Zhou, and M. Grayson, *J. Electron. Mater.* **44**, 2095 (2015).
- [31] L. Onsager, *Phys. Rev.* **37**, 405 (1931).
- [32] A. C. Smith, J. F. Janak, and R. V. Adler, *Electronic Conduction in Solids* (McGraw-Hill, 1967).
- [33] M. Buttiker, *Phys. Rev. Lett.* **57**, 1761 (1986).
- [34] S. Datta, *Electronic Transport in Mesoscopic Systems* (Cambridge University Press, 1995).
- [35] C. Liu, W. Chen, Y. Tao, J. Yang, and Y. Chen, *Int. J. Heat Mass Transf.* **121**, 72 (2018).
- [36] C. Hua and A. J. Minnich, *Phys. Rev. B* **90**, 214306 (2014).
- [37] L. D. Landau and E. M. Lifshitz, *Statistical Physics: Vol 1* (Pergamon Press, 1980), p. 427.
- [38] Z. Chen, Z. Wei, Y. Chen, and C. Dames, *Phys. Rev. B* **87**, 125426 (2013).
- [39] S. Lee, F. Yang, J. Suh, S. Yang, Y. Lee, G. Li, H. Sung Choe, A. Suslu, Y. Chen, C. Ko, J. Park, K. Liu, J. Li, K. Hippalgaonkar, J. J. Urban, S. Tongay, and J. Wu, *Nat. Commun.* **6**, 8573 (2015).
- [40] H. Jang, J. D. Wood, C. R. Ryder, M. C. Hersam, and D. G. Cahill, *Adv. Mater.* **27**, 8017 (2015).
- [41] B. Sun, X. Gu, Q. Zeng, X. Huang, Y. Yan, Z. Liu, R. Yang, and Y. K. Koh, *Adv. Mater.* **29**, 1603297 (2017).
- [42] J. Zhu, H. Park, J. Y. Chen, X. Gu, H. Zhang, S. Karthikeyan, N. Wendel, S. A. Campbell, M. Dawber, X. Du, M. Li, J. P. Wang, R. Yang, and X. Wang, *Adv. Electron. Mater.* **2**, 1600040 (2016).

- [43] A. Jain and A. J. H. McGaughey, *Sci. Rep.* **5**, 8501 (2015).
- [44] H. Yuan, X. Liu, F. Afshinmanesh, W. Li, G. Xu, J. Sun, B. Lian, A. G. Curto, G. Ye, Y. Hikita, Z. Shen, S. C. Zhang, X. Chen, M. Brongersma, H. Y. Hwang, and Y. Cui, *Nat. Nanotechnol.* **10**, 707 (2015).
- [45] M. N. Ozisik, *Boundary Value Problems of Heat Conduction* (Courier Corporation, 2013), p. 460.
- [46] Y. Chen, C. Chen, R. Kealhofer, H. Liu, Z. Yuan, L. Jiang, J. Suh, J. Park, C. Ko, H. S. Choe, J. Avila, M. Zhong, Z. Wei, J. Li, S. Li, H. Gao, Y. Liu, *J. Analytis*, Q. Xia, M. C. Asensio, and J. Wu, *Arxiv* **1805**, 00418v1 (2018).
- [47] J. P. Feser, J. Liu, and D. G. Cahill, *Rev. Sci. Instrum.* **85**, 104903 (2014).
- [48] V. Mishra, C. L. Hardin, J. E. Garay, and C. Dames, *Rev. Sci. Instrum.* **86**, 54902 (2015).
- [49] A. T. Ramu and J. E. Bowers, *Rev. Sci. Instrum.* **83**, 124903 (2012).
- [50] Y. S. Ju, K. Kurabayashi, and K. E. Goodson, *Thin Solid Films* **339**, 160 (1999).